

# Characterizing the Strong Earth Gravity Prior

Björn Jörges<sup>1\*</sup> and Joan López-Moliner<sup>2</sup>

<sup>1</sup> Center for Vision Research, York University, 4700 Keele Street, Toronto, ON M3J 1P3, Canada

<sup>2</sup> Vision and Control of Action (VISCA) group, Department of Cognition, Development and Psychology of Education, Institut de Neurociències, Universitat de Barcelona, Ps. Vall d'Hebron 171, 08035 Barcelona, Catalonia, Spain.

\* Corresponding Author

## Abstract

Humans expect downwards moving objects to accelerate and upwards moving objects to decelerate. These results have been interpreted as humans maintaining an internal model of gravity. We have previously suggested an interpretation of these results within a Bayesian framework of perception: earth gravity could be represented as a Strong Prior that overrules noisy sensory information (Likelihood) and therefore attracts the final percept (Posterior) very strongly. Based on this framework, we use published data from a timing task involving gravitational motion to determine the mean and the standard deviation of the Strong Earth Gravity Prior. To get its mean, we refine a model of mean timing errors we proposed in a previous paper (Jörges & López-Moliner, 2019), while expanding the range of conditions under which it yields adequate predictions of performance. This underscores our previous conclusion that the gravity prior is likely to be very close to  $9.81 \text{ m/s}^2$ . To obtain the standard deviation, we identify different sources of sensory and motor variability reflected in timing errors. We then model timing responses based on quantitative assumptions about these sensory and motor errors for a range of standard deviations of the

earth gravity prior, and find that a standard deviation of around  $2 \text{ m/s}^2$  makes for the best fit. This value is likely to represent an upper bound, as there are strong theoretical reasons along with supporting empirical evidence for the standard deviation of the earth gravity being lower than this value.

## Introduction

There is ample evidence that humans represent earth gravity and use it for a variety of tasks such as interception (Ceccarelli et al., 2018; La Scaleia, Zago, Moscatelli, Lacquaniti, & Viviani, 2014; J McIntyre, Zago, & Berthoz, 2001; Mijatovic, La Scaleia, Mercuri, Lacquaniti, & Zago, 2014; Senot et al., 2012; Zago et al., 2004a, 2004b; Zago, La Scaleia, Miller, & Lacquaniti, 2011; Zago & Lacquaniti, 2005a; Zago, McIntyre, Senot, & Lacquaniti, 2008), time estimation (Moscatelli & Lacquaniti, 2011), the perception of biological motion (Maffei et al., 2015) and many more. Recently, we have shown that gravity-based prediction for motion during an occlusion matched performance under a  $1g$  expectation not only qualitatively, but also quantitatively (Jörges & López-Moliner, 2019). This was an important finding to support our interpretation of the above results as a strong prior in a Bayesian framework of perception (Jörges & López-Moliner, 2017). The results presented in (Jörges & López-Moliner, 2019) indicate that temporal errors in a timing task were consistent with a mean of  $1g$  ( $9.81 \text{ m/s}^2$ ) when occlusions were long enough. In the present paper, we extend the simulations brought forward in our previous paper: First, we consider how accounting for the Aubert-Fleischl effect, which leads humans to perceive moving object at about 80% of their actual speed when they pursue the target with their eyes (Aubert, 1887; Dichgans, Wist, Diener, & Brandt, 1975; Fleischl, 1882), can extend our simple  $1g$ -based model to shorter occlusions. Furthermore, to fully characterize a prior, we need to not only indicate its mean, but also its standard deviation. The second goal of the present paper is thus to determine the standard deviation of the strong gravity prior. We aim to achieve this goal by simulations based on assumptions about the different sources of noise relevant to the task at hand.

45 In this paper, we adopt a constructivist-computational framework (Marr, 1982; Nanay, 2014); we view  
 46 perception as a process by which humans acknowledge the state of the world around us based on both  
 47 prior knowledge and sensory online information in order to guide their interactions with the external  
 48 world. Please note that other psychological traditions, such as ecological perception (Gibson, 1986), deny  
 49 the necessity of prior knowledge. Within our constructivist framework, we envision (visual) perception as  
 50 a two-step process: Encoding and Decoding (Gold & Shadlen, 2007; Schneidman, Bialek, & Li, 2003). During  
 51 Encoding, low level signals such as luminosity, retinal velocities or orientation are picked up by the  
 52 perceptual system and represented as neural activity. However, these low-level sensory signals, and the  
 53 neural activity they are represented as, can be ambiguous with respect to the state of the world: for  
 54 example, the same retinal velocities can correspond to vastly different physical velocities, depending on  
 55 the distance between observer and object. An object that moves 6 m in front of the observer in the fronto-  
 56 parallel plane with a physical speed of 1 m/s elicits a retinal speed of about 9.5°/s when fixation is  
 57 maintained. The same retinal speed could correspond to a target that moves at a physical speed of 1.2 m/s  
 58 7 m in front of the observer. Decoding is the process of interpreting optic flow information. In Decoding,  
 59 humans often combine sensory input with previous (prior) knowledge to obtain a more accurate and  
 60 precise estimate of the observed state of the world. For example, we use knowledge about the size of an  
 61 object to recover its most likely distance to the observer, thus providing a key to recover its physical  
 62 velocity from retinal motion. If we, for example know that we are observing a basketball and know from  
 63 experience that its radius is 0.12 m, and we perceive that the target occupies a visual angle of 0.5°, we  
 64 know that the target moves at 7 m in front of us. We then also know that the physical velocity of the ball  
 65 is 1.2 m/s, not 1 m/s. In some, if not many instances, this combination occurs according to Bayes' formula:

$$P(A|B) = \frac{P(B|A)P(A)}{P(B)} \quad [1]$$

The probability of a state of the world A given evidence B is the probability of observing evidence B given the state of the world A multiplied by the probability of the state of the world (A), divided by the probability of the evidence (B). In a Bayesian framework, sensory input (Likelihood), corresponding to the term  $\frac{P(B|A)}{P(B)}$  in Equation 1, and prior knowledge (Prior), corresponding to  $P(A)$  in Equation 1, are combined according to their respective precisions to yield a more precise and more accurate final percept (Posterior). Under many circumstances, Prior, Likelihood and Posterior can be represented as normal distributions whose standard deviations correspond to the representation's reliability. If an organism has a high sensitivity to the sensory input, that is, when they are able to reliably distinguish one stimulus strength from a very similar stimulus strength, the standard deviation of the Likelihood would be very low, which corresponds to a very narrow distribution. On the other hand, if the organism has a very precise representation of the most likely state of the world, the Prior would be very narrow. Finally, the standard deviation of the Posterior would depend on the precision of Likelihood and Prior. Usually, both the Prior and the Likelihood contribute to the Posterior; for example when we know that our opponent in a tennis match *usually* serves in the right corner of the court, but *not always*, (Prior) and we have good visibility of their serving motion, but since the motion is so quick, we do not have a lot of time to acquire evidence (Likelihood). We thus take sensory input (e. g. about their body posture while serving) into account only to some extent (see "Normal Prior" scenario in Figure 1). However, in the case of gravity it seems that the expectation of Earth Gravity overrules all sensory information that humans collect on the law of motion of an observed object (La Scaleia, Zago, & Lacquaniti, 2015; McIntyre et al., 2001; McIntyre, Zago, Berthoz, & Lacquaniti, 2003; Zago & Lacquaniti, 2005b; Zago et al., 2008). On a theoretical level, this is a sensible assumption, since all of human evolution and each human's individual development occurred under Earth Gravity. In Bayesian terms, the Prior is extremely precise and thus overrules all sensory information represented as the Likelihood. According to our interpretation, we would thus expect an extremely low value for the standard deviation of the earth gravity prior ("Strong Prior" scenario in Figure 1). We would

expect this value to be represented more precisely than linear velocities, which generally elicit Weber Fractions of 10%, which corresponds to a standard deviation of about 15% of the mean represented stimulation.

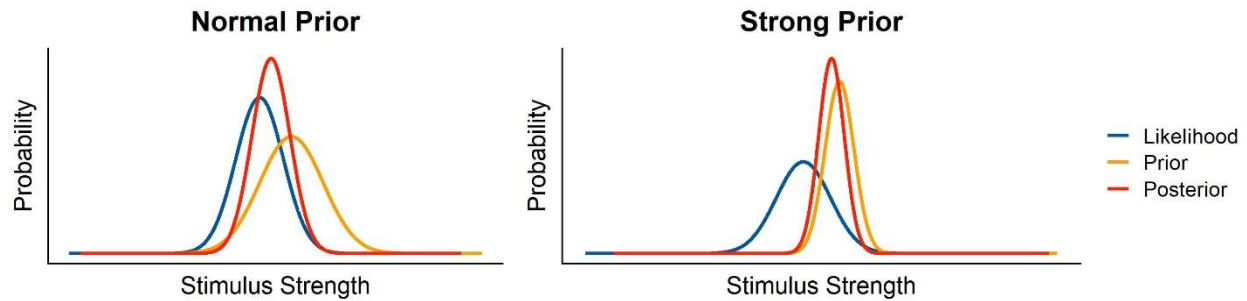


Figure 1: Graphical illustration of Likelihood, Prior and Posterior in a Bayesian framework, for both a normal, relatively shallow Prior, and a strong, extremely precise Prior.

In the following, we use the data from our previous study (Jörges & López-Moliner, 2019) to simulate the variability of responses under different assumptions about the standard deviation of the gravity prior.

## Methods

In this paper, we use previously published data (Jörges & López-Moliner, 2019). The pre-registration for the original hypotheses can be viewed on Open Science Foundation (<https://osf.io/8vg95/>). All data relevant to this project are available in our GitHub repository (<https://github.com/b-jorges/SD-of-Gravity-Prior>). We will thus only briefly repeat the most important experimental parameters. We showed participants tennis balls moving on parabolic trajectories in the fronto-parallel plane. The balls could have one out of 6 gravity levels (-1g, 0.7g-1.3g), one out of two initial vertical velocities and one out of two initial horizontal velocities. In trials with a positive gravity value (i.e., downwards acceleration), the target started with an upwards initial velocity component and vice-versa. The target disappeared early after peak

(Long Occlusion) or late after peak (Short Occlusion). Each combination of parameters was presented 24 times for a total of 1344 trials. Participants indicated by mouse click when they thought the target returned to its initial height. The stimulus was presented in an immersive 3D environment. **Error! Reference source not found.** provides a 2D illustration of visual scene and target trajectories.

## Results

We have reported mean difference in a previous paper (Jörges & López-Moliner, 2019). In the following, we thus limit ourselves to analyzing the influence of gravity on the *precision* of responses in preparation for the simulations we are conducting after. We used a slightly different, more liberal outlier analysis for this project to make sure that we don't lose any variability present in participants' responses. We also exclude all data collected from the author (s10; all 1344 trials). Further, we exclude all trials where subjects pressed the button before the target disappeared (38 trials) or where the temporal error was greater than 2 s (178 trials). Overall, we excluded 1.6% of all trials from the nine participants included in the analysis. To make it easier to compare temporal errors across conditions, we then computed the error ratio:

$$Error\ Ratio = \frac{Error + Occluded\ Duration}{Occluded\ Duration} \quad [4]$$

In Figure 2, we illustrate the response distributions. For an analysis and interpretation of the effect of gravitational motion on accuracy, please see our previous paper (Jörges & López-Moliner, 2019).

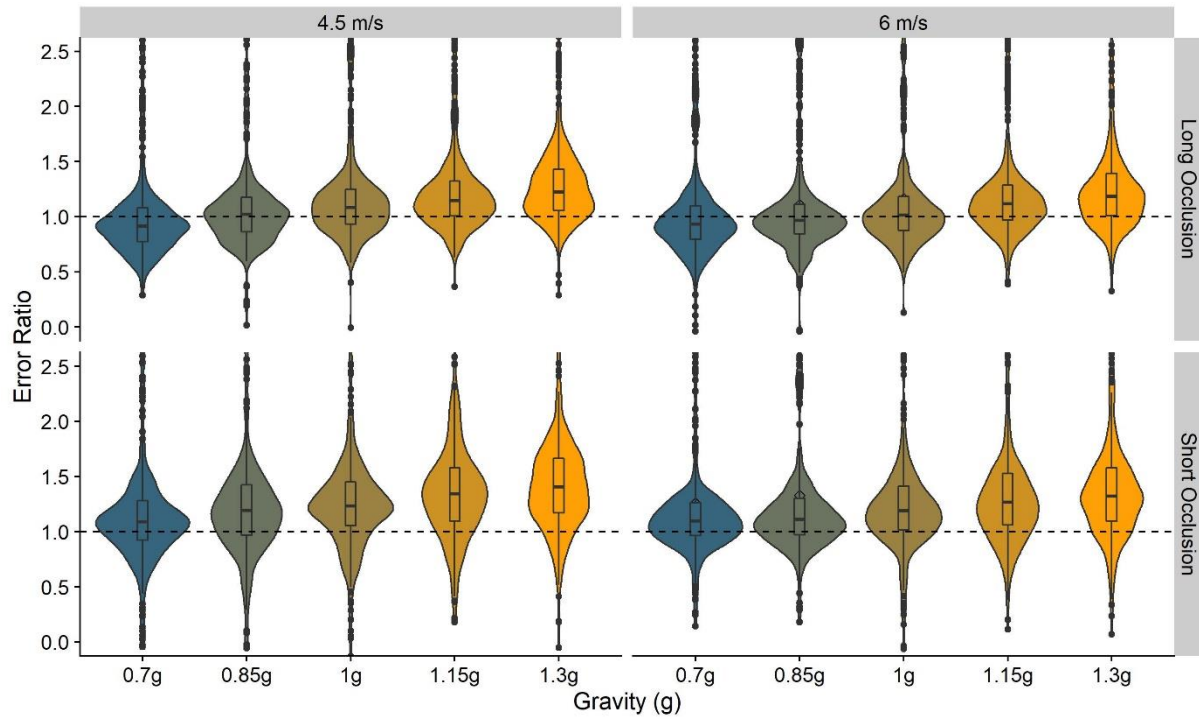


Figure 2: Temporal errors in the 0.7-1.3 g conditions. The wings of each structure indicate the distribution of responses, while the boxplot in the middle of each structure indicate the 75% percentiles and the mean per condition.

While we used Linear Mixed Modelling to assess accuracy, assessing precision differences between conditions is not straight-forward with this method. Therefore, we employ Bayesian Linear Mixed Modelling to assess whether gravity has an impact on the precision of the timing responses. The R package brms (Bürkner, 2018), which provides user-friendly interface for the package rstan (Stan Development Team, 2016), uses a very similar syntax to the more well-known lme4 (Bates, Mächler, Bolker, & Walker, 2015). In addition to mean differences, this type of analysis also allows us to test for variability differences between conditions. We thus fit a mixed model to explain both means and standard deviations of the response distributions, with gravity as a fixed effect and varying intercepts per participant as random effects. In lme4/brms syntax, the test model is specified as:

$$\text{Error Ratio} \sim \text{Gravity} + (1 | \text{Subject})$$

$$\text{Sigma} \sim \text{Gravity} + (1 | \text{Subject})$$

[5]

Where the first line corresponds to the statistical structure that corresponds to the means of the response distributions and the second line corresponds to the standard deviations of the response distributions. Unlike regular Linear Mixed Models, Bayesian Linear Mixed Models do not need to be compared to a Null Model. We can use the hypothesis() function from the R Core package (R Core Team, 2017) to test hypotheses directly. We found a posterior probability of >0.999 that a lower gravity value is related to lower variability, the sigma coefficient for Gravity being 0.057 (SE = 0.004; 95% Confidence

		0.7g-1.3 Block					-1g/1g Block	
		Long Occlusion						
$v_{yi}$		0.7g	0.85g	1g	1.15g	1.3g	-1g	1g
4.5 m/s	Mean	1.12	1.11	1.20	1.24	1.30	1.33	1.17
	SD	0.47	0.49	0.53	0.42	0.44	0.53	0.38
6 m/s	Mean	1.05	1.11	1.17	1.24	1.32	1.23	1.16
	SD	0.49	0.55	0.57	0.54	0.57	0.56	0.46
		Short Occlusion						
$v_{yi}$		0.7g	0.85g	1g	1.15g	1.3g	-1g	1g
4.5 m/s	Mean	1.22	1.31	1.34	1.41	1.52	1.68	1.35
	SD	0.64	0.65	0.65	0.56	0.88	0.86	0.58
6 m/s	Mean	1.26	1.33	1.37	1.47	1.49	1.51	1.35
	SD	0.65	0.77	0.77	0.88	0.75	0.80	0.76

Table 1: Means and standard deviations observed for the temporal errors divided by gravities and initial vertical velocities

Interval = [0.051;0.064]) in the log space. In the regular space, this corresponds to a standard deviation of 0.296 (95 % CI = [0.282;0.313]) for 0.7g, 0.321 (95% CI = [0.303;0.344]) for 0.85g, 0.350 (95% CI = [0.326;0.378]) for 1g, 0.382 (95% CI = [0.351;0.416]) for 1.15g and 0.413 (95% CI = [0.378;0.458]) for 1.3g. **Error! Reference source not found.** lists all mean temporal errors and the respective standard errors across participants. Note that, unlike the results from the Bayesian Mixed Model, the variability values from **Error! Reference source not found.** also include variability that the Mixed Model assigns to the individual.

Interestingly, precision seems to be higher for 1g trials than for -1g trials. To test this observation statistically, we fitted a second Bayesian Linear Mixed Model to the -1g/1g data, where gravity as fixed effect factor and subjects as random effects predict the timing error:



$$Error\ Ratio \sim Gravity + (1 |Subject)$$

We tested the hypothesis that Gravity would lead to lower variability. The posterior probability of this hypothesis being true was  $> 0.999$ , with a sigma coefficient for Gravity of  $-0.011$  (SE =  $0.004$ ; 95 % Confidence Interval =  $[-0.014, -0.009]$  in the log space. That is, the standard deviation of distribution of  $-1g$  responses in regular space is  $0.426$  (95% Confidence Interval =  $[0.414; 0.439]$ ), while the standard deviation of the distribution of  $1g$  responses in regular space is  $0.344$  (95% Confidence Interval =  $[0.334; 0.353]$ ). This indicates that the absolute error is lower and thus the precision is higher for  $1g$  than for  $-1g$ . On a theoretical level, this is in line with previous findings (Indovina et al., 2005) showing that the internal representation of gravity is not activated when upwards motion is presented, even when the absolute value of acceleration impacting the object is equal to the absolute value of earth gravity ( $9.81 \text{ m/s}^2$ ). The precision may thus be higher for  $1g$  than for  $-1g$  because the internal model of gravity is utilized for  $1g$ , but not for  $-1g$  trials.

## Simulations

The physical formula for distance from initial velocity and acceleration (Equation 4) is the base for both of our simulation procedures. This reflects the assumption that humans perform the task at hand accurately – under most circumstances. This assumption is supported by our data, which show a high accuracy for the earth gravity conditions.

We furthermore neglect the air drag for these simulations and use the equation for linearly accelerated motion as an approximation.

$$d_y = \frac{g}{2} * t^2 + v_y * t \quad [6]$$

$$t_{1/2} = \frac{-v_y \pm \left( v_y^2 - 4 * \frac{g}{2} * d_y \right)^{0.5}}{2 * \frac{g}{2}} \quad [7]$$

As evidenced by a comparison between equations (1) and (2) and equations (3) and (4), the computational complexity increases significantly if we want to accommodate air drag, while the gains in accuracy are marginal (0.02 s in the condition with the most extreme differences).

### Mean of the Gravity Prior

To characterize the mean Strong Gravity Prior, we build upon our model the mean timing errors presented in our previous data (Jörges & López-Moliner, 2019). Importantly, the predictions of our model matched the observed data only for the Long Occlusion condition. In the Long Occlusion condition, subjects displayed a tendency to respond slightly too late, while their responses should be centered around zero. Our ad hoc explanation of this discrepancy was that subjects were often executing a saccade when the ball returned to initial height, which may have interfered with the predictions (Jörges & López-Moliner, 2019). An alternative explanation may be, however, that our subjects underestimated the target's speed at disappearance due to the so called Aubert-Fleischl phenomenon: humans estimate the speed of a target that they pursue with their eyes at about 80% of its actual speed (Aubert, 1887; de Graaf, Wertheim, & Bles, 1991; Fleischl, 1882; Spering & Montagnini, 2011; Wertheim & Van Gelder, 1990). Our subjects were specifically instructed to follow the target with their eyes, and the eye-tracking data we collected that they generally did pursue the target (Jörges & López-Moliner, 2019). An underestimation of the velocity at disappearance could explain the tendency of subjects to respond too late in the Short Occlusion condition. For the Long Occlusion condition, on the contrary, the vertical speed at disappearance is very low and has a nearly neglectable influence on the final prediction. Setting the perceived velocity at 80% of the presented velocity should thus yield more accurate predictions for the

Short Occlusion condition, while the accuracy for the Long Occlusion condition would be largely maintained. We thus employ the same procedure laid out in (Jörges & López-Moliner, 2019), but add a coefficient of 0.8 to the perceived velocity at disappearance to account for the Aubert-Fleischl phenomenon.

We will briefly summarize the procedure and then present how this tweak affects the results of our simulations. We used the physical formula for distance from accelerated motion (Equation 4, with  $d$  being the height at disappearance,  $v_y$  the vertical velocity at disappearance and  $g$  being gravity). For our simulations, we assume that humans use an earth gravity value of  $9.81 \text{ m/s}^2$  independently of the presented gravity value, as long as the display is roughly in line with a real-world scenario. We furthermore assume that we perceive the vertical velocity at disappearance at 80% of the presented velocity. Equation 7 thus becomes

$$t_{1/2} = \frac{-v_{y,perceived} \pm \left( v_{y,perceived}^2 - 4 * \frac{g_{earth}}{2} * d_y \right)^{0.5}}{2 * \frac{g_{earth}}{2}} \quad [8]$$

With  $v_{y,perceived} = 0.8 * v_{y,presented}$  and  $g_{earth} = \frac{9.81 \text{ m}}{\text{s}^2}$ .

We use this formula to simulate the timing error for each trial separately without adding noise. We furthermore also simulate the responses without accounting for the Aubert-Fleischl phenomenon to compare performance for both models. Figure 3 shows the mean errors observed in our participants (“Obs. Error”), the mean errors when accounting for the Aubert-Fleischl phenomenon (“Sim. Error (AF)”), and the mean errors when not accounting for the Aubert-Fleischl phenomenon (“Sim. Error (No AF)”).

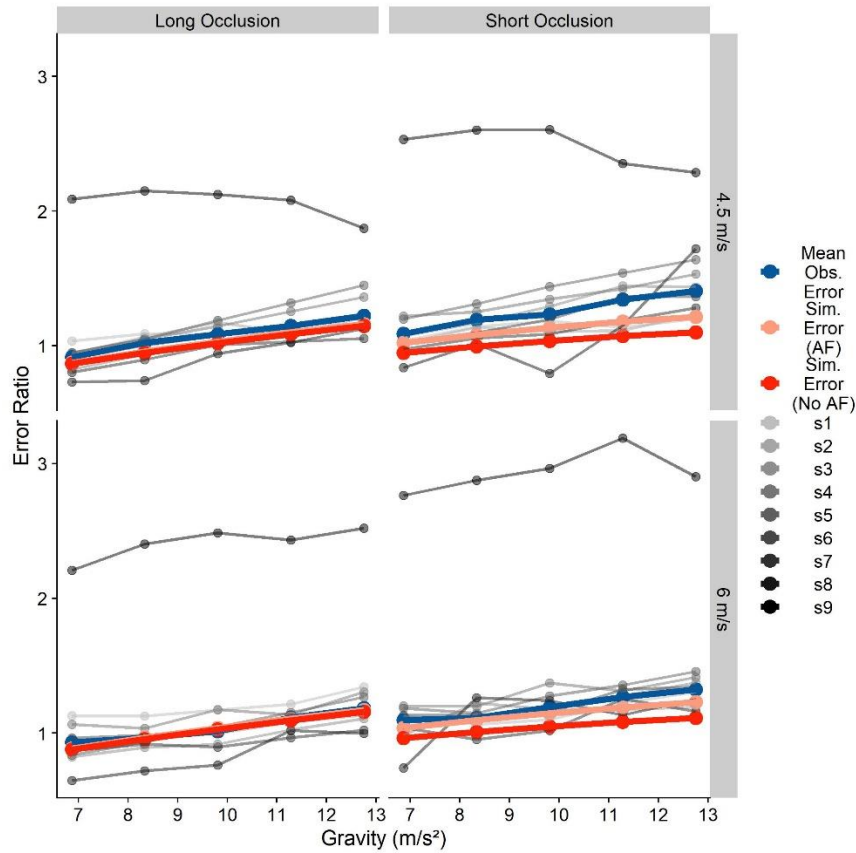


Figure 3: Mean temporal errors that we observed in our participants (across participants in blue, and for each participant separately in shades of grey), simulated taking the Aubert-Fleischl phenomenon into account (light red) and simulated without taking the phenomenon into account for the different conditions. The right column represents values for the Long Occlusion condition, while the left column represents the Short Occlusion condition. The upper row shows values for an initial vertical velocity of 4.5 m/s, while the lower row represents initial vertical velocities of 6 m/s. Note that the standard errors for the observed errors are so small that all error bars fall well within the area covered by the dots.

The overall Root Mean Squared Error between AF model predictions and observed behavior is 0.2, and for the non-AF model predictions substantially higher, at 0.265. Table 2 shows the error for each of the conditions. Including the AF phenomenon thus vastly improves the model's generalizability.

	Long Occlusion		Short Occlusion	
$v_{yi}$	<i>AF</i>	<i>No AF</i>	<i>AF</i>	<i>No AF</i>
4.5 m/s	0.150	0.160	0.236	0.333
6 m/s	0.148	0.158	246	0.344

Table 2: Root Mean Squared Errors (RMSEs) between simulated and observed mean errors for simulations including the Aubert-Fleischl phenomenon (AF) and simulations that don't (No AF). Lower values signify a better fit.

This improvement upon our previous model lends further support to the idea that the mean of a strong gravity prior is at or very close to  $9.81 \text{ /s}^2$ .

## Standard Deviation of the Gravity Prior

The second value needed to characterize a normal distribution, which we assume the strong gravity prior to be represented as, is its standard deviation. There are two different ways to approach this problem: First, we can simulate the temporal responses of our subjects assuming different standard deviations for the gravity prior and minimize the difference between the standard deviations of the responses we observed in our subjects and the model standard deviations. In this case, we would draw the values for  $v_y$ ,  $d_y$  and  $g_{earth}$  from distributions with given means and standard deviations, and compute a simulated temporal response from these values. The mean for  $v_y$  would be the last observed velocity in y direction, corrected by a factor of 0.8 for the Aubert-Fleischl phenomenon, and the standard deviation can be computed based on Weber fractions for velocity discrimination from the literature. The mean for  $d_y$  is the distance in y direction between the point of disappearance and the reference height. The mean for  $g_{earth}$  is  $9.81 \text{ m/s}^2$ , and we optimize over its standard deviation to match the standard deviation observed in the subjects' temporal responses.

A second approach would be to solve equation (3) for  $g_{earth}$ , and then compute its mean and standard deviation analytically based on the means and standard deviations of  $t$ ,  $v_y$  and  $d_y$ . For the addition, subtraction and multiplication of two normal distributions, there are analytic solutions to compute mean and standard deviation of the resulting distribution.

$$g_{earth} = \frac{2(d_y - v_y * t)}{t^2} \quad [8]$$

However, as evident from Equation 5, this method requires computing the standard deviation of the quotient of two distributions. To our knowledge, this is not possible in an analytical fashion and would entail simulations by itself. We will thus focus on the simulation approach.

## Assumptions

For this approach, we need to make several assumptions. In the following, we will outline each and provide the rationale for the chosen values. Please note that we conduct these simulations in absolute terms (i.e., absolute errors) to mimic the processes more closely, but convert quality metrics (such as model fits) and results into relative terms (i. e., error ratios).

**Use of Equation (3)** – In our previous paper, we have shown that predictions based on Equation 3 fit observed temporal errors reasonably well (Jörges & López-Moliner, 2019). This is particularly the case when subjects extrapolated motion for larger time frames in the Long Occlusion condition. The difference in predictions for this equation with regards to Equation (2) is at most 3 ms, and the added computational complexity does not justify the added accuracy, especially since our main concern is precision.

$v_y$  – The velocity term in Equation 4 ( $v_y * t$ ) refers to the part of the full distance the target moved because of its initial velocity. Our targets disappeared right after peak, therefore their initial velocity was very low. The velocity term thus contributes less to the full estimate than the gravity term, especially in

the Long Occlusion condition (see also Figure 4C). Importantly, the vertical velocity component is not perceived directly. Rather, it has to be recovered from the tangential speed ( $v_{tan,perceived}$ ) and the angle between the tangential speed vector and the vertical speed vector ( $\alpha_{perceived}$ ) by means of the equation:

$$v_{y,perceived} = \cos(\alpha_{perceived}) * v_{tan,perceived} \quad [9]$$

Weber fractions for the discrimination of angular velocities reported in the literature are about 10% (Kaiser, 1990). To calculate the standard deviation of the distribution of perceived velocities from the Weber fraction, we have to find that normal distribution where a difference of 10% from its mean leads to a proportion of responses of 25/75%. For a standardized normal distribution with a mean of 1, this is a standard deviation of 0.148. Note that, by using a standardized normal distribution, we assume that Weber fractions are constant across the relevant range of stimulus strengths. Figure 4C shows how predictions vary with varying variability in perceived vertical velocity: The effect is negligible for the Long Occlusion condition, while it increases response variability uniformly across gravities. Further variability is incurred in estimating  $\alpha_{perceived}$ . Following (Schoups, Vogels, & Orban, 1995), the JND for orientation discrimination in untrained subjects is around 6° for oblique orientations. This corresponds to a standard deviation of 0.089.

Furthermore, we need to account for the Aubert-Fleischl phenomenon, which consists in an underestimation of the velocity of a moving target during smooth pursuit (Aubert, 1887; de Graaf et al., 1991; Fleischl, 1882; Spering & Montagnini, 2011; Wertheim & Van Gelder, 1990). While this effect should in principle be partially offset by improved predictions for motion coherent with earth gravity – an empirical question that has, to our knowledge, not been addressed so far –, our simulations show that a Aubert-Fleischl correction factor of 0.8 yields an excellent fit for the observed mean errors. We thus proceed with a value of 0.8 also for the simulations concerning the standard deviation.

281  $d_y$  – For the distance term ( $d_y$ ), we choose the stimulus value as mean distance, as we don't expect any  
282 biases. In terms of precision, Weber fractions of 3% to 5% are observed for distance estimates in the front  
283 parallel plane (Norman, Todd, Perotti, & Tittle, 1996). However, since subjects have to estimate the  
284 distance not between two well defined points, but rather the height above the simulated table, the  
285 precision of these estimates is likely lower than reported for the above task. We thus work with a Weber  
286 fraction of twice the reported value (10%). Using the above method, we determine that the standard  
287 deviation for this value is 0.148. Figure 4A shows how predictions vary with variability in perceived  
288 distance: There is a slight logarithmic pattern, where response variability added by higher variability in  
289 perceived distance increases with decreasing gravity.

290  $t$  – The response time  $t$  is measured directly in our task, both in mean and variability.

291 **Remaining Variability** – For our simulations, we rely on accounting for every source of variability in the  
292 responses. One source of error beyond perceiving and representing  $g$ ,  $v_y$  and  $d_y$  is the motor response.  
293 Motor responses are likely to vary strongly between tasks, for which reason variability reported in the  
294 literature is of limited use. To estimate the error introduced by these further factors, we thus take  
295 advantage of previous results indicating that the gravity model is not activated for upside-down motion  
296 (Indovina et al., 2005), a hypothesis which is also supported by our data.



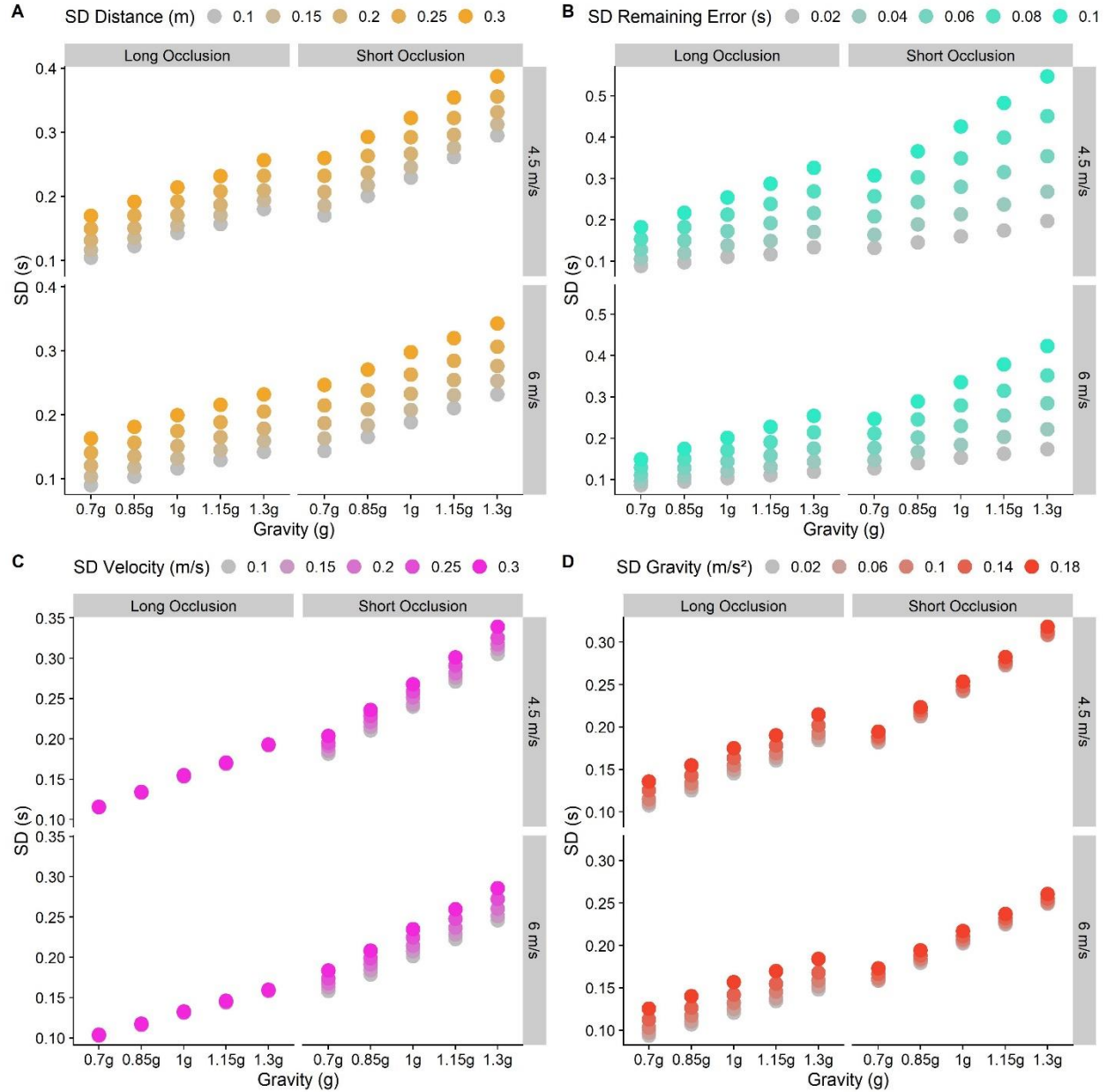


Figure 4: Predictions for different standard deviations chosen for different parameters in our model. Dots represent the standard deviation for each gravity (0.7g-1.3g), divided by Occlusion category (Long and Short) and initial vertical velocities (4.5 and 6 m/s). The color gradient indicates different values of the (standardized) standard deviation for the perceived distance, the perceived velocity, the represented gravity and the remaining error. The baseline values are 0.148 for distance and velocity, 0.1 for gravity and 0.05 for the remaining (motor) error. A. Predictions for five standardized standard deviations for the perceived distance (0.1-0.3 m). B. Predictions for five standard deviations for the remaining (motor) error (0.02-0.1 s), modelled as independent of and constant across initial velocities, gravities and occlusion conditions. C. Predictions for five different standardized standard deviations for the last perceived velocity (0.1-0.3 m/s). D. Predictions for five different standardized standard deviations for the represented gravity (0.02-0.18 m/s<sup>2</sup>).

Under this assumption, we can use the responses for the inverted gravity condition to estimate the errors introduced by motor variability. An inactivation of the gravity prior would mean that the gravity acting

upon the object should be represented with the same precision as arbitrary gravities. We previously found Weber fractions of between 13% and beyond 30% for arbitrary gravities (Jörges, Hagenfeld, & López-Moliner, 2018), which is in line with those found for linear accelerations (Werkhoven, Snippe, & Alexander, 1992). We thus proceed with a value of 20%, which corresponds to a normalized standard deviation of 0.295 (see procedure above).

There are further constraints: First, the motor variability should be lower than the overall variabilities observed for the absolute error in each condition (the minimum is just over 0.08 s for the short occlusion condition with 1.3g and an initial vertical velocity of 4.5 m/s). Second, the motor variability should be equal across conditions and be independent of gravity, initial velocity and Occlusion category (see Figure 4B).

We put these values for  $\mathbf{g}$ ,  $\mathbf{v}_y$  and  $\mathbf{d}_y$  into Equation 4 to stimulate the temporal responses for each trial 1000 times. We minimize the Root Mean Square Errors (RMSE) between the standard deviations of the simulated timing error and the observed timing errors, separately for each combination of gravity, initial vertical velocity, Occlusion condition and participant. We collapsed the error across initial horizontal velocities because results for both values were virtually the same, mostly likely because the horizontal velocity barely influences overall flight duration in the presence of air drag, and not at all in the absence of air drag. After visualizing a relevant range of candidate values for the standard deviation of the remaining errors (see Figure 5), we use the `optim()` function implemented in R with a lower bound of 0.01 s and an upper bound of 0.06 s to find the best fit for the observed data. We found the best fit for a standard deviation of 0.058 s, with an RMSE of 0.04.

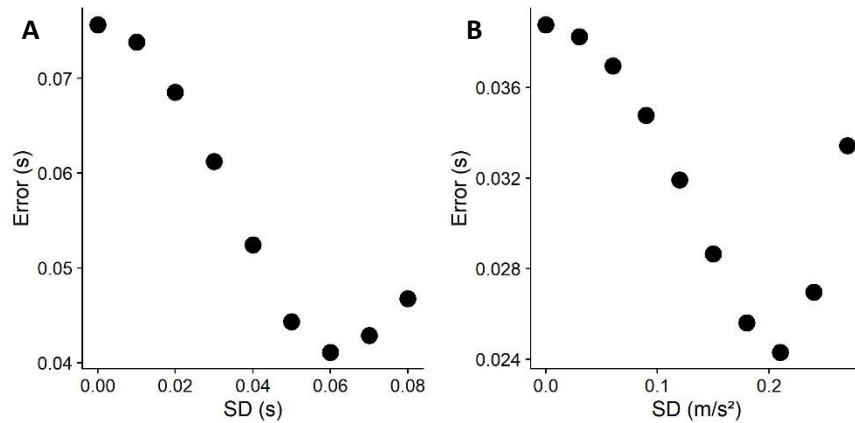


Figure 5: A. Root mean square errors (RMSE) between the standard deviation of timing errors simulated based on different motor errors (between 0.00 and 0.07 s) and the standard deviation of observed timing errors. B. Root mean square errors (RMSE) between the standard deviation of timing errors simulated based on different standard deviations of the gravity prior between 0.15 and  $0.25 \times 9.81 \text{ m/s}^2$  and the standard deviation of observed timing errors.

## The Standard Deviation of the Gravity Prior

We then proceed to apply these values to simulate data sets based on the above assumptions, get the standard deviations for the timing error and compare them to standard deviations of the observed timing errors (Method 1). We restrict this comparison to the 0.7g/0.85g/1g/1.15/1.3g condition, as we expect the gravity model not to be activated for inverted gravitational motion. For a discussion of factors impacting the performance of the model for short occlusions, see (Jörges et al., 2018). We first simulate a range of sensible standard deviations (from 0, corresponding to an impossibly precise representation, to 0.28, corresponding to a quite imprecise representation with limited impact on the final percept, in steps of 0.03) to determine the lower and upper bounds of the optimization interval (see **Error! Reference source not found.**); Figure 4D furthermore highlights how changes in the simulated variability of the represented gravity changes response variability.

We find the errors to be lowest around 0.21, and choose thus 0.16 as the lower bound and 0.26  $\text{m/s}^2$  as the upper bound. We then search for that standard deviation that minimizes the error between simulated

and observed timing errors, using the `optim()` function implemented in R (R Core Team, 2017). For each iteration, we simulate 1000 data sets and minimize the Root Mean Square Error (RMSE) between the standard deviations of simulated and observed timing errors across these 1000 data sets. The R code we used for these simulations can be found on GitHub (<https://github.com/b-jorges/SD-of-Gravity-Prior>), including extensive annotations. We found a normalized standard deviation of 0.208 for the gravity prior, which corresponds to a standard deviation of about  $2.04 \text{ m/s}^2$  for a mean of  $9.81 \text{ m/s}^2$ , and a Weber fraction of 14.1%. The RMSE is 0.024. In Figure 6, we illustrate how the simulated standard deviations relate to the observed ones. The light red dots correspond to this method ("Simulated (Method1)"); as evident from the figure, the fits are better for the Long Occlusion condition, while the SDs are generally overestimated for the Short Occlusion condition.

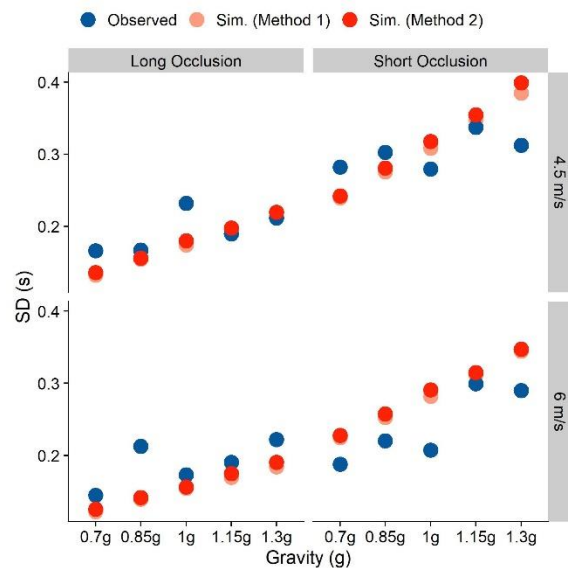


Figure 6: Observed and Simulated Standard Deviations separated by Occlusion Condition, initial vertical velocity and presented gravity. Blue indicates the observed standard deviations across subjects, while the standard deviations simulated through the two-step process (Method 1) are coded light red and the standard deviations simulated through the two-parameter fit (Method 2) are coded solid red.

If the gravity prior was discarded completely for upwards motion, we might observe even larger errors for -1g motion. We elaborate on this issue in the discussion. As there is thus some reason to believe that the gravity prior is not completely inactive in upwards motion, which may bias to above method to

overestimate the standard deviation of the gravity prior, we furthermore conducted simulations where both the motor variability and the strong gravity prior are fitted to the data (Method 2). To this end, we use the `optimize()` function implemented in R which uses the Nelder and Mead method (Nelder & Mead, 1965) to determine those values for the motor standard deviation and the standard deviation of the gravity prior that yield the smallest errors between simulated and observed variability. This is suitable because variability in the gravity prior and motor variability affect the final variability differentially (see Figure 4): a higher motor variability leads to uniformly higher standard deviations for the observed error, while a higher gravity variability affects longer trajectories (Long Occlusion, higher initial vertical velocity and lower gravities) more strongly than shorter ones. Based on above results, we chose 0.04 and 0.2 as starting parameters, but did not limit the parameter space. This method allots variability in slightly different proportions: the standard deviation for the motor error is 0.06 s and the standardized standard deviation of the gravity prior is 0.211 (which corresponds to a non-standardized standard deviation of 2.07 m/s<sup>2</sup> and a Weber fraction of 14.2%), with an RMSE of 0.024. These values are extremely close to the values found with Method 1. While it is worth noting that fitting both parameters to the data makes this method more susceptible to overfitting, this lends additional support to the tentative conclusion that the standard deviation of the gravity prior is just above 2 m/s<sup>2</sup> or a Weber Fraction of 14.2%. The simulated standard deviations for these conditions are depicted in solid red in the Figure 8 ("Simulated (Method 2)"): The fits are much better for the long occlusions, at the cost of a slight overestimation of the variability for the short occlusions.

## Discussion

Humans assume in many tasks and circumstances that objects in their environment are affected by earth gravity. It has thus been suggested that we maintain a representation of this value, which we then recruit

to predict the behavior of objects in our environment. We recently interpreted this representation as a Strong Prior in a Bayesian framework (Jörges & López-Moliner, 2017). A “Strong Prior” is a prior with a reliability so high that it overrules any sensory input represented in the likelihood. Based on data from timing task (previously reported in Jörges & López-Moliner, 2019), we make an attempt at determining the standard deviation of a hypothetical Strong Earth Gravity Prior. Our general approach is to account for other sources of perceptuo-motor variability in the task based on thresholds reported in the literature, and attributing the remaining variability to the Gravity Prior. Based on this approach, we find a standard deviation of  $2.13 \text{ m/s}^2$  (Method 1) or  $2.07 \text{ m/s}^2$  (Method 2), for a prior with a mean of  $9.81 \text{ m/s}^2$ , which corresponds – mathematically – to a Weber fraction of 14.1% or 14.2%, respectively. This is considerably lower than Weber fractions generally observed for acceleration discrimination, but above Weber fractions for the discrimination of constant speeds (McKee, 1981).

Interestingly, when we simulated the timing errors with a fixed value of  $9.81 \text{ m/s}^2$  (i. e. in a non-Bayesian framework where the value of earth gravity is not represented as a distribution, but rather a value set at  $1g$ ; see Jörges & López-Moliner, 2019 and also above), we found that our results fit the observed timing error quite nicely for each gravity value. That is, the observed gravity (corresponding to the Likelihood) had no discernable influence on the final percept (Posterior). However, in a Bayesian framework, this is only possible if the Likelihood is extremely shallow and the Prior is extremely precise. A Weber fraction of about 30% for the likelihood (which we assume for acceleration discrimination), and a Weber fraction of 14.1% or 14.2% for the prior (as modelled) would not result in discarding the likelihood completely (see also Figure 1; even for a strong prior and a rather shallow likelihood, the likelihood attracts the posterior to some extent). Our results thus reveal a mismatch between the means observed in our experiment, the modelled standard deviation and a Bayesian explanation.

We see two possible ways to explain this mismatch. Firstly, our observed standard deviation for the gravity prior could be an upper bound. Our method relies on identifying all sources of variability and allotting

variability in the response accordingly. Since we did not measure our participants' Weber fractions for velocity and distance discriminations individually, but rather used averages reported in the literature for somewhat different tasks, this may have distorted how much variability perceived distances and velocity at disappearance introduced in the response. Furthermore, when estimating the variability introduced in the motor response, we part from the premise that the internal model of gravity is not activated at all for -1g motion. However, we observe a bias to respond too late in this condition, suggesting that humans expect objects to accelerate less when moving upwards. This could be taken as evidence that the internal model of gravity is still activated to some extent. In this case, we would need to allot more variability to the motor error, which in turn would lead to a lower standard deviation for the gravity prior. However, this pattern in our data is also consistent with humans taking arbitrary accelerations into account insufficiently in perceptuo-motor tasks, which has been reported repeatedly for tasks where the gravity prior is highly unlikely to be recruited (Benguigui, Ripoll, & Broderick, 2003; Bennett & Benguigui, 2013; Brenner et al., 2016; Werkhoven et al., 1992). The values of 14.1% or 14.2% obtained above may thus be an upper bound for the standard deviation of the Earth Gravity Prior.

A second possibility is that prior knowledge and online perceptual input are combined in a non-Bayesian fashion (and we should thus avoid the terminology "Prior", "Likelihood" and "Posterior"), where the mean of the final percept is set according to an acceleration of  $9.81 \text{ m/s}^2$ , while its standard deviation is determined by a (not necessarily Bayesian) combination of prior knowledge and online sensory information.

## Conclusion

In this paper, we build upon a simple model for coincidence timing of gravitational motion brought forward in (Jörges & López-Moliner, 2019). By accounting for the Aubert-Fleischl phenomenon, we extend

the domain of our model to also include shorter extrapolation intervals. Furthermore, we propose a procedure to determine the standard deviation of a potential gravity prior, and apply it to pre-existing data from a timing task. Standard deviations of  $2.13 \text{ m/s}^2$  or  $2.07 \text{ m/s}^2$  (depending on the method) explains the behavior observed in our task best. However, considering the literature we would expect an even lower standard deviation, as a Prior with a mean of  $9.81 \text{ m/s}^2$  and standard deviations of  $2.13 \text{ m/s}^2$  or  $2.07 \text{ m/s}^2$  should not attract the Posterior as strongly as has been commonly observed. We thus believe that we are not able to fully disentangle different sources of noise in our data; the value we find for the standard deviation of the earth gravity prior is thus more likely an upper bound, and follow-up experiments may find lower values.

#### Author Contributions and Notes

BJ conducted the simulations and wrote the paper. BJ and JLM established the research question in a joint effort. JLM provided advice at every step of the project.

The authors declare no conflict of interest.

#### Acknowledgments

Funding was provided by the Catalan government (2017SGR-48) and the project ref. PSI2017-83493-R from AEI/Feder, UE. The first author (BJ) was supported by the Canadian Space Agency (CSA).

#### References

Aubert, H. (1887). Die Bewegungsempfindung. *Pflüger, Archiv Für Die Gesamte Physiologie Des*



458        *Menschen Und Der Thiere*, 40(1), 459–480. <https://doi.org/10.1007/BF01612710>

459    Bates, D., Mächler, M., Bolker, B. M., & Walker, S. C. (2015). Fitting linear mixed-effects models using  
460        lme4. *Journal of Statistical Software*, 67(1). <https://doi.org/10.18637/jss.v067.i01>

461    Benguigui, N., Ripoll, H., & Broderick, M. P. (2003). Time-to-contact estimation of accelerated stimuli is  
462        based on first-order information. *Journal of Experimental Psychology. Human Perception and*  
463        *Performance*, 29(6), 1083–1101. <https://doi.org/10.1037/0096-1523.29.6.1083>

464    Bennett, S. J., & Benguigui, N. (2013). Is Acceleration Used for Ocular Pursuit and Spatial Estimation  
465        during Prediction Motion? *PLoS ONE*, 8(5). <https://doi.org/10.1371/journal.pone.0063382>

466    Brenner, E., Rodriguez, I. A., Muñoz, V. E., Schootemeijer, S., Mahieu, Y., Veerkamp, K., ... Smeets, J. B. J.  
467        (2016). How can people be so good at intercepting accelerating objects if they are so poor at  
468        visually judging acceleration? *I-Perception*, 7(1), 1–13. <https://doi.org/10.1177/2041669515624317>

469    Bürkner, P. C. (2018). Advanced Bayesian multilevel modeling with the R package brms. *R Journal*, 10(1),  
470        395–411. <https://doi.org/10.32614/rj-2018-017>

471    Ceccarelli, F., La Scaleia, B., Russo, M., Cesqui, B., Gravano, S., Mezzetti, M., ... Zago, M. (2018). Rolling  
472        motion along an incline: Visual sensitivity to the relation between acceleration and slope. *Frontiers*  
473        *in Neuroscience*, 12(JUN), 1–22. <https://doi.org/10.3389/fnins.2018.00406>

474    de Graaf, B., Wertheim, A. H., & Bles, W. (1991). The Aubert-Fleischl paradox does appear in visually  
475        induced self-motion. *Vision Research*, 31(5), 845–849. [https://doi.org/10.1016/0042-](https://doi.org/10.1016/0042-6989(91)90151-T)  
476        6989(91)90151-T

477    Dichgans, J., Wist, E., Diener, H. C., & Brandt, T. (1975). The Aubert-Fleischl phenomenon: A temporal  
478        frequency effect on perceived velocity in afferent motion perception. *Experimental Brain Research*,  
479        23(5), 529–533. <https://doi.org/10.1007/BF00234920>

480 Fleischl, V. (1882). Physiologisch-optische Notizen. *Sitzungsberichte Der Akademie Der Wissenschaften*  
481 *Wien*, (3), 7–25.

482 Gibson, J. J. (1986). *The Ecological Approach to Visual Perception*. New York: Taylor & Francis.

483 Gold, J. I., & Shadlen, M. N. (2007). *The Neural Basis of Decision Making*.  
484 <https://doi.org/10.1146/annurev.neuro.29.051605.113038>

485 Indovina, I., Maffei, V., Bosco, G., Zago, M., Macaluso, E., & Lacquaniti, F. (2005). Representation of  
486 visual gravitational motion in the human vestibular cortex. *Science (New York, N.Y.)*, 308(April),  
487 416–419. <https://doi.org/10.1126/science.1107961>

488 Jörges, B., & López-Moliner, J. (2019). Earth-Gravity Congruent Motion Facilitates Ocular Control for  
489 Pursuit of Parabolic Trajectories. *Scientific Reports*, 9(1). [https://doi.org/10.1038/s41598-019-](https://doi.org/10.1038/s41598-019-50512-6)  
490 50512-6

491 Jörges, Björn, Hagenfeld, L., & López-Moliner, J. (2018). The use of visual cues in gravity judgements on  
492 parabolic motion. *Vision Research*, 149, 47–58. <https://doi.org/10.1016/J.VISRES.2018.06.002>

493 Jörges, Björn, & López-Moliner, J. (2017). Gravity as a Strong Prior: Implications for Perception and  
494 Action. *Frontiers in Human Neuroscience*, 11(203). <https://doi.org/10.3389/fnhum.2017.00203>

495 Jörges, Björn, & López-Moliner, J. (2019). Earth-Gravity Congruent Motion Facilitates Ocular Control for  
496 Pursuit of Parabolic Trajectories. *Scientific Reports*, 9(1), 1–13. [https://doi.org/10.1038/s41598-](https://doi.org/10.1038/s41598-019-50512-6)  
497 019-50512-6

498 Kaiser, M. K. (1990). Angular velocity discrimination. *Perception & Psychophysics*, 47(2), 149–156.  
499 <https://doi.org/10.3758/BF03205979>

500 La Scaleia, B., Zago, M., & Lacquaniti, F. (2015). Hand interception of occluded motion in humans: A test

501 of model-based versus on-line control. *Journal of Neurophysiology*, 114, 1577–1592.  
502 <https://doi.org/10.1152/jn.00475.2015>

503 La Scaleia, B., Zago, M., Moscatelli, A., Lacquaniti, F., & Viviani, P. (2014). Implied dynamics biases the  
504 visual perception of velocity. *PLoS ONE*, 9(3). <https://doi.org/10.1371/journal.pone.0093020>

505 Maffei, V., Indovina, I., Macaluso, E., Ivanenko, Y. P., Orban, G. A., & Lacquaniti, F. (2015). Visual gravity  
506 cues in the interpretation of biological movements: Neural correlates in humans. *NeuroImage*,  
507 104(October 2014), 221–230. <https://doi.org/10.1016/j.neuroimage.2014.10.006>

508 Marr, D. (1982). A computational investigation into the human representation and processing of visual  
509 information.pdf. *Vision: A Computational Investigation into the Human Representation and*  
510 *Processing of Visual Information*.

511 McIntyre, J, Zago, M., & Berthoz, A. (2001). Does the Brain Model Newton’s Laws. *Nature Neuroscience*,  
512 12(17), 109–110. <https://doi.org/10.1097/00001756-200112040-00004>

513 McIntyre, Joseph, Zago, M., Berthoz, A., & Lacquaniti, F. (2003). The Brain as a Predictor: On Catching  
514 Flying Balls in Zero-G. In J. C. Buckey & J. L. Homick (Eds.), *The Neurolab Spacelab Mission:*  
515 *Neuroscience Research in Space* (pp. 55–61). National Aeronautics and Space Administration,  
516 Lyndon B. Johnson Space Center.

517 McKee, S. P. (1981). A local mechanism for differential velocity detection. *Vision Research*, 21(4), 491–  
518 500. [https://doi.org/10.1016/0042-6989\(81\)90095-X](https://doi.org/10.1016/0042-6989(81)90095-X)

519 Mijatovic, A., La Scaleia, B., Mercuri, N., Lacquaniti, F., & Zago, M. (2014). Familiar trajectories facilitate  
520 the interpretation of physical forces when intercepting a moving target. *Experimental Brain*  
521 *Research*, 232(12), 3803–3811. <https://doi.org/10.1007/s00221-014-4050-6>

522 Moscatelli, A., & Lacquaniti, F. (2011). The weight of time: Gravitational force enhances discrimination of

523 visual motion duration. *Journal of Vision*, 11(4), 1–17. <https://doi.org/10.1167/11.4.1>

524 Nanay, B. (2014). The Representationalism versus Relationalism Debate: Explanatory Contextualism  
525 about Perception. *European Journal of Philosophy*, 23(2), 321–336.  
526 <https://doi.org/10.1111/ejop.12085>

527 Nelder, J. A., & Mead, R. (1965). A Simplex Method for Function Minimization. *The Computer Journal*,  
528 7(4), 308–313. <https://doi.org/10.1093/comjnl/7.4.308>

529 Norman, J. F., Todd, J. T., Perotti, V. J., & Tittle, J. S. (1996). The Visual Perception of Three-Dimensional  
530 Length. *Journal of Experimental Psychology: Human Perception and Performance*, 22(1), 173–186.  
531 <https://doi.org/10.1037/0096-1523.22.1.173>

532 R Core Team. (2017). *A Language and Environment for Statistical Computing*. R Foundation for Statistical  
533 Computing,. Retrieved from <http://www.r-project.org/>.

534 Schneidman, E., Bialek, W., & Li, M. J. B. (2003). *Synergy, Redundancy, and Independence in Population*  
535 *Codes*. 23(37), 11539–11553.

536 Schoups, A. A., Vogels, R., & Orban, G. A. (1995). Human perceptual learning in identifying the oblique  
537 orientation: retinotopy, orientation specificity and monocularly. *The Journal of Physiology*, 483(3),  
538 797–810. <https://doi.org/10.1113/jphysiol.1995.sp020623>

539 Senot, P., Zago, M., Le Seac'h, a., Zaoui, M., Berthoz, a., Lacquaniti, F., & McIntyre, J. (2012). When Up  
540 Is Down in Og: How Gravity Sensing Affects the Timing of Interceptive Actions. *Journal of*  
541 *Neuroscience*, 32(6), 1969–1973. <https://doi.org/10.1523/JNEUROSCI.3886-11.2012>

542 Spering, M., & Montagnini, A. (2011). Do we track what we see? Common versus independent  
543 processing for motion perception and smooth pursuit eye movements: A review. *Vision Research*,  
544 51(8), 836–852. <https://doi.org/10.1016/j.visres.2010.10.017>

545 Stan Development Team. (2016). *Stan: the R interface to Stan. R package version 2.14.1*. 1–23. Retrieved  
 546 from <http://mc-stan.org>

547 Werkhoven, P., Snippe, H. P., & Alexander, T. (1992). Visual processing of optic acceleration. *Vision*  
 548 *Research*, 32(12), 2313–2329. [https://doi.org/10.1016/0042-6989\(92\)90095-Z](https://doi.org/10.1016/0042-6989(92)90095-Z)

549 Wertheim, A. H., & Van Gelder, P. (1990). An acceleration illusion caused by underestimation of stimulus  
 550 velocity during pursuit eye movements: Aubert-Fleischl revisited. *Perception*, 19(4), 471–482.  
 551 <https://doi.org/10.1068/p190471>

552 Zago, M., Bosco, G., Maffei, V., Iosa, M., Ivanenko, Y., & Lacquaniti, F. (2004a). Internal Models of Target  
 553 Motion: Expected Dynamics Overrides Measured Kinematics in Timing Manual Interceptions.  
 554 *Journal of Neurophysiology*, 91(4), 1620–1634. <https://doi.org/10.1152/jn.00862.2003>

555 Zago, M., Bosco, G., Maffei, V., Iosa, M., Ivanenko, Y. P., & Lacquaniti, F. (2004b). Fast Adaptation of the  
 556 Internal Model of Gravity for Manual Interceptions: Evidence for Event-Dependent Learning.  
 557 *Journal of Neurophysiology*, 93(2), 1055–1068. <https://doi.org/10.1152/jn.00833.2004>

558 Zago, M., La Scaleia, B., Miller, W. L., & Lacquaniti, F. (2011). Coherence of structural visual cues and  
 559 pictorial gravity paves the way for interceptive actions. *Journal of Vision*, 11(10), 1–10.  
 560 <https://doi.org/10.1167/11.10.13.Introduction>

561 Zago, M., & Lacquaniti, F. (2005a). Cognitive, perceptual and action-oriented representations of falling  
 562 objects. *Neuropsychologia*, 43(2 SPEC. ISS.), 178–188.  
 563 <https://doi.org/10.1016/j.neuropsychologia.2004.11.005>

564 Zago, M., & Lacquaniti, F. (2005b). Internal Model of Gravity for Hand Interception: Parametric  
 565 Adaptation to Zero-Gravity Visual Targets on Earth. *Journal of Neurophysiology*, 94(2), 1346–1357.  
 566 <https://doi.org/10.1152/jn.00215.2005>

567 Zago, M., McIntyre, J., Senot, P., & Lacquaniti, F. (2008). Internal models and prediction of visual  
568 gravitational motion. *Vision Research*, 48(14), 1532–1538.  
569 <https://doi.org/10.1016/j.visres.2008.04.005>

570

571